Published in final edited form as:
Aging Cell. 2010 August ; 9(4): 536–544. doi:10.1111/j.1474-9726.2010.00581.x.

Age-Dependent Cardiomyopathy in Mitochondrial Mutator Mice is Attenuated by Overexpression of Catalase Targeted to Mitochondria

Dao-Fu Dai[1], **Tony Chen**[1], **Jonathan Wanagat**[5], **Michael Laflamme**[1], **David J. Marcinek**[2,3], **Mary J Emond**[4], **Calvin P. Ngo**[1], **Tomas A. Prolla**[6], and **Peter S. Rabinovitch**[1]

[1]Department of Pathology, University of Washington, Seattle, WA 98195

[2]Department of Radiology, University of Washington, Seattle, WA 98195

[3]Department of Bioengineering, University of Washington, Seattle, WA 98195

[4]Department of Biostatistics, University of Washington, Seattle, WA 98195

[5]Department of Medicine, Division of Geriatrics, David Geffen School of Medicine at UCLA, CA

[6]Departments of Genetics & Medical Genetics, University of Wisconsin-Madison, WI 53706

Abstract

Mitochondrial defects have been found in aging and several age-related diseases. Mice with a homozygous mutation in the exonuclease encoding domain of mitochondrial DNA polymerase gamma ($Polg^{m/m}$) are prone to age-dependent accumulation of mitochondrial DNA mutations and have shown a broad spectrum of aging-like phenotypes. However, the mechanism of cardiac phenotypes in relation to the role of mitochondrial DNA mutations and oxidative stress in this mouse model has not been fully addressed. We demonstrate age-dependent cardiomyopathy in $Polg^{m/m}$ mice, which by 13-14 months of age displays marked cardiac hypertrophy and dilatation, impairment of systolic and diastolic function and increased cardiac fibrosis. This age-dependent cardiomyopathy is associated with increases in mitochondrial DNA (mtDNA) deletions and protein oxidative damage, increased expression of apoptotic and senescence markers, as well as a decline in signaling for mitochondrial biogenesis. The relationship of these changes to mitochondrial reactive oxygen species (ROS) was tested by crossing $Polg^{m/m}$ mice with mice that overexpress mitochondrial targeted catalase (mCAT). All of the above phenotypes were partially rescued in $Polg^{m/m}$/mCAT mice. These data indicate that accumulation of mitochondrial DNA damage with age can lead to cardiomyopathy, and that this phenotype is partly mediated by mitochondrial oxidative stress.

Keywords

mitochondria; mutation; aging; cardiomyopathy; oxidative stress

Introduction

Mitochondria are the primary sites regulating cellular metabolism and performing numerous tasks such as the Krebs cycle, as well as metabolism of fatty acids, steroids and amino acids. However, the most crucial function is energy production through the electron transport chain

Correspondence: Peter S. Rabinovitch, MD, PhD. Professor, Department of Pathology University of Washington 1959 Pacific Ave NE, HSB-K081 Seattle, WA 98195 Phone: 206-685-3761; Fax: 206-616-8271 petersr@u.washington.edu .

and oxidative phosphorylation. Intracellular reactive oxygen species (ROS) are produced in the mitochondria as a consequence of electron flux through the electron transport chain. Because of their proximity to this source of ROS, mitochondrial proteins, lipids and nucleic acids are believed to be primary targets of oxidative damage during oxidative stress, causing mitochondrial DNA (mtDNA) damage and mitochondrial dysfunction, which might cause further production of ROS that eventually leads to cell death and organ dysfunction (reviewed in (Balaban *et al*. 2005)). It has been documented that mtDNA point mutations and deletions accumulate with age in various tissues in humans and rodents (Corral-Debrinski *et al*. 1992; Wanagat *et al*. 2002; Khaidakov *et al*. 2003). Mice with homozygous proofreading-deficient mutation of polymerase gamma ($Polga^{D257A/D257A}$, abbreviated as $Polg^{m/m}$) were previously shown to have shortened lifespan, with median survival of 416 days and maximum survival of 460 days (Trifunovic *et al*. 2004; Kujoth *et al*. 2005). A striking "premature aging" phenotype was noted starting at 7-9 months of age, which include alopecia, graying, kyphosis and osteoporosis, sarcopenia (loss of muscle mass) and presbycusis (age-related hearing loss). This is concomitant with a dramatic increase in mtDNA point mutation and deletion frequencies (Vermulst *et al*. 2007). We previously showed that while both point mutations and deletions in mtDNA accumulate with age in $Polg^{m/m}$ mice, mtDNA deletions are better correlated with the phenotypes in these mice (Vermulst *et al*. 2008). In the heart, Zhang et al reported that mice with cardiac-specific transgene of a proofreading-deficient mitochondrial Polg (D181A) displayed enlarged heart with chamber dilatation and increased apoptosis starting at 4 weeks of age, and these phenotypes could be rescued by Cyclosporin A (Zhang *et al*. 2003; Mott *et al*. 2004).Though the mitochondrial free radical theory of aging proposes that a vicious cycle between increased mtDNA damage and mitochondrial ROS production is causal to aging, the initial characterization of $Polg^{m/m}$ mice did not reveal any significant increase in oxidative damage. Instead, the phenotypes in this animal model were correlated with the induction of apoptotic markers (Mott *et al*. 2001; Kujoth *et al*. 2005).

We have previously demonstrated that cells from mice overexpressing catalase targeted to the mitochondria (mCAT) are better protected from ROS injury to mitochondria and have an approximately 20% extension of median and maximum lifespan (Schriner *et al*. 2005). This phenotype was not seen in mice with overexpression of catalase targeted to peroxisomes (pCAT, the normal location of catalase), suggesting that mitochondrial ROS (mtROS) plays an especially important role in mammalian aging. We have subsequently shown that mCAT attenuates cardiac aging phenotypes, including left ventricular hypertrophy, diastolic dysfunction, impairment of myocardial performance, ventricular fibrosis and cardiomyocyte hypertrophy, concomitant with reduction of the age-dependent increase in mitochondrial oxidative damage and mtDNA deletions (Dai *et al*. 2009). The heart is a vital organ rich in mitochondria with high oxygen consumption, and is especially prone to mitochondrial damage. Indeed, mitochondrial dysfunction has been implicated in congestive heart failure and defects in genes encoding mitochondrial enzymes are associated with idiopathic hypertrophic and dilated cardiomyopathies (DiMauro & Schon 2003). Furthermore, previous observations showed increased mtDNA deletions in several experimental models of heart failure (Marin-Garcia *et al*. 2001). However, the causal link between mtDNA deletions and cardiac dysfunction with aging is not well established.

In this report we investigate the effect of increased mtDNA mutations on age-dependent cardiac structural changes and functional disturbance using $Polg^{m/m}$ mice, and explore the contribution of mtROS in these mice by crossing mCAT to $Polg^{m/m}$ mice. We found age-dependent cardiomyopathy in $Polg^{m/m}$ mice in parallel with increases in cardiac mtDNA deletions, senescence and apoptotic markers and mitochondrial protein oxidative damage, all of which were attenuated in $Polg^{m/m}$ mice expressing mCAT. This study indicates that primary damage to mtDNA can cause cardiomyopathy, with cardiac hypertrophy,

remodeling and dysfunction that is even more severe than natural cardiac aging, and is partly mediated by increased mtROS.

Results

Age-dependent cardiac hypertrophy and dysfunction in Polg$^{m/m}$ mice is ameliorated by mCAT overexpression

Echocardiography was performed to evaluate cardiac structure and function in young (4-6 months) and older (13-14 months) Polg$^{m/m}$, Polg$^{m/m}$/mCAT mice as well as their wild type (WT) and mCAT littermates. We found that Polg$^{m/m}$ mice have an age-dependent cardiomyopathy which is more severe than the usual cardiac aging phenotype. Although young Polg$^{m/m}$ mice had a moderate increase in left ventricular mass index (LVMI, $p<0.025$) compared to WT littermates, older Polg$^{m/m}$ mice had marked cardiac hypertrophy, with an approximately 2-fold increase in LVMI compared with WT littermates ($p<0.001$; Fig.1A). Systolic function measured by fractional shortening (FS) was significantly depressed by 13% compared with WT littermates (Fig.1B). Older Polg$^{m/m}$ mice had significant impairment of myocardial performance as shown by increased myocardial performance index, indicating an increased fraction of time with ineffective LV ejection (Fig.1C), as well as increased diastolic dysfunction (defined as $Ea/Aa < 1$; Fig.1D). All of the above age-related pathology was significantly ameliorated in 13-14 months old Polg$^{m/m}$/mCAT mice. In older Polg$^{m/m}$ mice the LV chamber was significantly enlarged by 21% at end-diastolic phase and by 31% at end-systolic phase (Fig.1E and 1F), indicating cardiac remodeling; however, this cardiac chamber enlargement was more prominent than that observed in usual cardiac aging, even at 26-33 months of age. Furthermore, cardiac hypertrophy and impairment of systolic as well as diastolic function in 13-14 months old Polg$^{m/m}$ mice was even more severe than that of WT 26-33 month old mice, as documented in our previous studies (Dai *et al*. 2009).

Both young and older Polg$^{m/m}$ mouse hearts showed cardiac enlargement: young Polg$^{m/m}$ mice had a 24% greater heart weight / tibia length than WT littermate controls, increasing to 38% greater in older Polg$^{m/m}$ mice (Fig. 2A and F). This is consistent with the echocardiographic findings of increased wall thickness and chamber enlargement (Fig.1). Myocyte hypertrophy was also apparent in both age groups, but was much greater in older Polg$^{m/m}$ mice, which showed an approximately 25% greater median fiber width than WT littermate controls (Fig.2B and G). Both the heart weight and fiber width changes were significantly ameliorated in older Polg$^{m/m}$/mCAT mice ($P<0.01$ for both). Interestingly, Polg$^{m/m}$ mouse hearts demonstrated substantial heterogeneity in myocardial fiber width, as shown by a wider interquartile range with larger number of massively hypertrophied cardiomyocytes (shown by the outlier points above the boxplot), especially in older Polg$^{m/m}$ mice (Fig. 2G). This finding is consistent with the mosaic pattern of age-related mitochondrial disease, in which the cellular phenotype depends on mitochondrial mutation load and occurs only when mtDNA mutations exceed a certain threshold of heteroplasmy (Herbst *et al*. 2007). As shown in Fig. 2C, interstitial fibrosis was increased in older Polg$^{m/m}$ mouse ventricles. We also found scattered foci of replacement fibrosis (Fig.2D), patches of fibrosis that arise to replace dying cardiomyocytes, as seen in several types of cardiomyopathies. Areas of replacement fibrosis are known to have reduced conduction velocity due to reduced connexins expression, and increasing susceptibility to arrhythmia (Stein *et al*. 2008; Saffitz 2009). In contrast, older Polg$^{m/m}$/mCAT mouse hearts showed only mild interstitial and perivascular fibrosis (Fig.2E). Quantitative analysis of the blue area representing fibrous tissue in Masson's Trichrome stained histological sections demonstrated an age-dependent increase in ventricular fibrosis in Polg$^{m/m}$ mouse hearts, which was significantly attenuated in the mCAT mice ($P<0.05$; Fig. 2H). Increased ventricular fibrosis in Polg$^{m/m}$ mice was confirmed by elevated procollagen type 1a2 gene

expression, an essential component of cardiac fibrosis. This effect was also ameliorated by mCAT (*P*=0.11 for young, *P*=0.02 for older, Fig.2I).

Mitochondrial DNA deletions and oxidative damage are increased in older Polg$^{m/m}$ hearts

Using a quantitative PCR method (Vermulst *et al*. 2008), we measured mtDNA deletion frequencies in the common deletion site in the major arc of the mitochondrial genome. Consistent with our previous report (Vermulst *et al*. 2008), we found an age-dependent accumulation of mtDNA deletions in both WT and Polg$^{m/m}$ mouse hearts. The Polg$^{m/m}$ mice showed a greatly accelerated frequency of mtDNA deletion, with a 40-fold increase in mtDNA deletions in 13-14 months old Polg$^{m/m}$ hearts compared to young WT mice and a 10-fold increase compared to WT littermates (Fig. 3A). MtDNA deletions were substantially reduced in older Polg$^{m/m}$/mCAT mice compared to Polg$^{m/m}$ littermates (*P*=0.01). This mCAT protective effect provides direct evidence that the accumulation of mtDNA damage with age in these mitochondrial mutator mice is at least partially mediated by an increase in mtROS.

To evaluate oxidative damage to mitochondria, we measured mitochondrial protein carbonyl content, an indicator of protein oxidative damage. We found a 19% increase in mitochondrial protein carbonyls in older Polg$^{m/m}$ compared with WT littermates (*P*=0.05, Fig.3B). This was significantly reduced by mCAT overexpression (*P*=0.03, Fig. 3B).

Senescence and apoptosis in older Polg$^{m/m}$ mouse hearts was attenuated by mCAT overexpression

The p16^{INK4a} tumor suppressor protein is an inhibitor of cyclin dependent kinases that has been shown to be a useful marker of senescence and aging in mice and humans (Krishnamurthy *et al*. 2004; Ressler *et al*. 2006). Although all groups of young mice showed low p16^{INK4a} gene expression, and there was very little, if any increase in expression in 13-14 month WT mice, we found an approximately 3-fold increase in p16^{INK4a} gene expression in older Polg$^{m/m}$ mouse hearts compared with WT littermates (Fig. 4A). The p16^{INK4a} gene expression was partially reduced in Polg$^{m/m}$/mCAT mouse hearts (*P*=0.03), consistent with an interaction between p16^{INK4a}, ROS and aging (Collado *et al*. 2007).

Mitochondrial dysfunction can lead to the activation of the intrinsic (mitochondrial) apoptotic pathway by releasing pro-apoptotic proteins such as cytochrome c and the opening of mitochondrial permeability transition pore (mPTP) and the collapse of mitochondrial membrane potential (Szalai *et al*. 1999). In the cytosol these drive the assembly of caspase complexes to form apoptosome and subsequent activation of caspase-3, a key effector of apoptosis. We thus examined the activation of caspase-3 by Western blot. There was a significant age-dependent increase in cleaved caspase-3 in WT mice (*P*<0.01, Fig 4B). Cleaved caspase-3 levels in young Polg$^{m/m}$ were higher than that in WT littermates (*P*<0.01) and comparable to that of older WT mice. Older Polg$^{m/m}$ showed more than a 5-fold increase compared with older WT littermates (*P*<0.01), and this was partially protected by mCAT (*P*=0.04, Fig 4B).

Mitochondrial biogenesis in Polg$^{m/m}$ mice and the effect of mCAT

Peroxisome proliferator-activated receptor (PPAR) gamma co-activator (PGC-1α) has been shown to be an important mediator of mitochondrial biogenesis, regulating factors that include nuclear respiratory factors (NRFs) and mitochondrial transcription factor A (TFAM), both of which transcribe genes for mitochondrial biogenesis (Wu *et al*. 1999; Arany *et al*. 2005). Oxidative stress and impaired mitochondrial function have been shown to directly activate the transcription of PGC-1a (St-Pierre *et al*. 2006); thus, increased mitochondrial damage by ROS or DNA mutations are expected to result in increased

signaling for mitochondrial biogenesis. As shown in Figure 5, there was significant increase in PGC-1α, TFAM and NRFs in young $Polg^{m/m}$ mouse hearts when compared with those of young WT mice. $Polg^{m/m}$/mCAT mice were significantly protected from this effect, suggesting that reduction of mitochondrial ROS by mCAT prevents activation of mitochondrial biogenesis. In contrast, the signaling for mitochondrial biogenesis significantly declined in older $Polg^{m/m}$ mouse hearts compared to young WT hearts, despite the accumulation of mitochondrial damage demonstrated above. The decline in mitochondrial biogenesis in older $Polg^{m/m}$ is partly ameliorated by mCAT, as shown by better preservation of PCG1α (P=0.018) and TFAM (P=0.09, Fig.5).

Discussion

MtDNA mutations and deletions have been observed in cardiac aging (Dai *et al*. 2009) and several forms of cardiomyopathy in humans (DiMauro & Schon 2003). Whether this DNA damage is the cause or consequence of cardiac aging and cardiomyopathy remains unclear. The current study provides direct evidence that primary damage to mtDNA, which accumulates with age in the mitochondrial mutator mouse heart, can cause myopathic changes, including cardiac hypertrophy, fibrosis and chamber enlargement, as well as impairment of systolic and diastolic function. Since the $Polg^{m/m}$ mutation is not cardiac-specific, a contribution by secondary factors such as anemia must also be considered. However, the pattern of cardiac injury observed in the $Polg^{m/m}$ does not suggest such a mechanism. We observed diffuse interstitial fibrosis and scattered microscopic foci of replacement fibrosis, rather than the circumferential, subendocardial scarring that is characteristic of anemia or global hypoxia. Moreover, the mutant hearts showed low, rather than high, contractility (fractional shortening) by echocardiography, which is inconsistent with a high cardiac output secondary to anemia. In sum, both the anatomic and functional findings were suggestive of a primary cardiomyopathy, rather than indirect cardiac injury.

Previous studies have reported “premature or accelerated aging” by showing several phenotypes that recapitulate aging in 7-9 months old $Polg^{m/m}$ mice (Trifunovic *et al*. 2004; Kujoth *et al*. 2005). We found that cardiomyopathy in middle age (13-14 mo) mitochondrial mutator mice is even more severe than in usual cardiac aging. Notably, cardiac hypertrophy at this age in $Polg^{m/m}$ mice is at least 50% greater than that previously observed in mice at least twice this age (26-33 months old) (Dai *et al*. 2009). Furthermore, the LV chamber was significantly enlarged in 13-14 mo $Polg^{m/m}$ mice, indicating cardiac remodeling, a finding not obviously seen in usual cardiac aging in mice (Figure 1) and humans (Lakatta & Levy 2003).

Due to its proximity to ROS production and the lack of histone protection, mtDNA is more susceptible to oxidative damage than nuclear DNA. Furthermore, repair of oxidative damage to mtDNA is carried out mainly by base excision repair (BER), which is initiated by the excision of inappropriate base by DNA glycosylase, then the resulting apurinic / apyrimidinic site is cleaved by AP endonuclease, followed by excision of 5′-deoxyribose-5-phosphate (dRP) ends by dRP lyase and filling of the gap by DNA polymerase. In mitochondria the latter two steps are solely dependent on Polg (Hansen *et al*. 2006). As previously shown, and confirmed in this study, $Polg^{m/m}$ mouse hearts have marked accumulation of mtDNA deletions with age (Fig. 3A). Although the accumulation of mtDNA deletions was reported to be better correlated with the shortened lifespan and the phenotypes of heterozygous and homozygous Polg mutant mice (Vermulst *et al*. 2008), a recent study reported that the absolute level of mtDNA deletions in these mice is quite low compared with the level of point mutations (Kraytsberg *et al*. 2009), therefore, both mtDNA deletions and point mutations should be considered in this setting. Kujoth *et al* (2005) did not find a significant increase in oxidative stress markers in 9 month old $Polg^{m/m}$ mice,

although there was a trend towards elevated mitochondrial protein carbonyls. We found that cardiac mitochondrial protein carbonyls were increased in 13-14 month old $Polg^{m/m}$ mice when compared to WT littermates (P=0.05, Figure 3B). To directly test the role of mtROS, we generated mice with both $Polg^{m/m}$ and mCAT expression. We found that mCAT significantly reduced mt-protein carbonyl content and mtDNA deletions, concomitant with attenuation of cardiomyopathy and all associated molecular markers in the older $Polg^{m/m}$ mouse hearts. One likely mechanism of cardioprotection by mCAT is the reduction of ROS-induced BER and a consequent reduction in mtDNA mutations produced by exonuclease-defective $Polg^{m/m}$ mice. However, the fact that mCAT did not completely rescue the phenotype of $Polg^{m/m}$ mice indicates that ROS-independent pathways are also involved, including, presumably, consequences of mutations to mtDNA introduced during replication by exonuclease defective Polg ($Polg^{m/m}$).

Cellular senescence is a state of permanent growth arrest that can be induced by a variety of stresses including DNA-damage and oxidative stress. The $p16^{INK4a}$ tumor suppressor protein, an inhibitor of cyclin dependent kinases CDK4 and CDK6, induces cellular senescence by imposing a G1 cell cycle arrest (Collado *et al*. 2007). Although the exact molecular mechanism responsible for the increased expression of $p16^{INK4a}$ in aging are not well understood, one plausible mechanism is oxidative damage and activation of the p38 MAPK pathway (Wang *et al*. 2002). Ito *et al*. reported that increased ROS activates the expression of the $p16^{INK4a}$ through p38 MAPK activation and this limits the function of hematopoetic stem cells (Ito *et al*. 2006). In addition, $p16^{INK4a}$ has been shown to interact with mitogenic signaling to increase ROS and activate protein kinase C-δ, which further promotes ROS generation and cellular senescence (Takahashi *et al*. 2006). This self-sustaining activation loop might explain the links between $p16^{INK4a}$, ROS and cellular senescence (Ramsey & Sharpless 2006). We have previously demonstrated a critical role of mtROS in cardiac aging (Dai *et al*., 2009). Accumulation of mtDNA damage with age in $Polg^{m/m}$ mice likely amplifies this relationship, as it was previously shown to produce defective respiratory enzymes (Vermulst *et al*. 2008(Metodiev *et al*. 2009). Such damage could in turn increase ROS production and amplify the $p16^{INK4a}$ / PKC-δ / ROS activation loop. Our observation that the $Polg^{m/m}$ phenotype is attenuated by mCAT provides a direct confirmation that it is at least partially mediated through mtROS. Thus, a second mechanism of protection by mCAT is likely to be by breaking the vicious cycle of oxidative damage to the electron transport chain and activation of signaling loops that are otherwise amplified in $Polg^{m/m}$ mice.

Mitochondria are important checkpoints of the apoptotic cell death. Several pathological stimuli, such as Ca^{2+} overload (Scorrano *et al*. 2003), ATP depletion and ROS (Hockenbery *et al*. 1993), have been shown to trigger the opening of mPTP and subsequent leakage of pro-apoptotic proteins. Consistent with the previous study by Kujoth *et al*., we found marked increase in apoptotic marker cleaved caspase-3 in $Polg^{m/m}$ mouse hearts, which was partly ameliorated by mCAT (Fig. 4B). This indicates that activation of apoptotic pathway in mitochondrial mutator mice is at least partly dependent on mtROS. However, mtROS is not necessarily involved from the very beginning, as they might be involved later in the pathway, such as through mPTP induction and cardiolipin oxidation, which result in cytochrome c release (Orrenius *et al*. 2007). The role of mPTP induction was demonstrated by a previous study showing that Cyclosporin A, an inhibitor of mPTP opening, attenuated apoptosis and cardiac dilatation in mitochondrial mutator mice (Mott *et al*. 2004). The residual apoptotic activity in $Polg^{m/m}$/mCAT mice implies that the induction of apoptosis also involved non-ROS mediated pathways, which might be related to direct damage to mitochondrial proteins secondary to mtDNA mutation.

As the master regulator of mitochondrial biogenesis and respiration, PGC-1α is regulated by several signaling pathways: calcium-dependent (calcineurin, calmodulin-dependent kinase), nutrient-energy signaling pathways (AMP-dependent serine/threonine protein kinase, sirtuins) and oxidative stress (reviewed in (Ventura-Clapier *et al*. 2008)). Hydrogen peroxide has been shown to directly activate the PGC-1α promoter by the coactivation of transcription factor Cre-binding protein. Furthermore, PGC-1α induction is required for upregulation of cellular antioxidant systems in response to oxidative stress (St-Pierre *et al*. 2006). There were significant increases in PGC-1α and its downstream targets in young $Polg^{m/m}$ mouse hearts when compared with those of young WT (Figure 5), and this was attenuated by mCAT. The latter is consistent with the reduction in fibrosis, and trends towards protection of cardiac hypertrophy in $Polg^{m/m}$/mCAT mice (P=0.09 for LVMI and P=0.07 for myocardial fiber width); this suggests that protection against mtROS is beneficial even in young $Polg^{m/m}$ mice, although we failed to demonstrate any increase of mt-protein carbonyls in young $Polg^{m/m}$ mouse hearts (Fig. 3B). Interestingly, the increase of mitochondrial biogenesis signaling in young $Polg^{m/m}$ mouse hearts dramatically declined in the older $Polg^{m/m}$ mouse hearts (Fig. 5), concomitant with the progression of cardiomyopathy. This finding is in agreement with several reports showing the downregulation of PGC-1α in experimental heart failure models and failing human hearts (Goffart *et al*. 2004; Sebastiani *et al*. 2007). Finally, although the molecular mechanisms underlying the loss of PGC-1α in heart failure are not well understood, our studies suggest that the role of mtROS and mtDNA deletions in this mechanism should be carefully considered.

In summary, accumulation of mtDNA mutations with age in $Polg^{m/m}$ mice leads to an accelerated form of cardiomyopathy. The fact that this phenotype is partially rescued by mCAT suggests that the pathogenesis of this age-dependent mitochondrial cardiomyopathy is partly mediated by increased mitochondrial oxidative stress. This evidence reinforces the interpretation that mitochondrial DNA damage and ROS are important contributors to cardiac aging, and that these are also potentially important therapeutic targets for combating cardiac aging.

Methods

Animals

The $Polg^{m/m}$($Polga^{D257A/D257A}$) mice were provided by Dr.Tomas A. Prolla (University of Wisconsin, Madison). The B6.C3H-Tg(mCAT) 4033Wcl was used to generate double transgenic $Polg^{m/m}$/mCAT by crossing $Polg^{m/+}$/$mCAT^{+/-}$ to $Polg^{m/+}$/$mCAT^{+/-}$. The resulting littermates of WT, $mCAT^{+/-}$, $Polg^{m/m}$/$mCAT^{-/-}$ and $Polg^{m/m}$/$mCAT^{+/-}$ were included in the cohort as previously described. All mice included in this study were of C57/Bl6 background. Mice were fed regular chow diet (irradiated Picolab Rodent Diet 20 #5053, PMI Nutrition International, Brentwood, MO) and reverse osmosis water. They were kept in a barrier specific-pathogen-free facility maintained at 70-74°F, 45-55% humidity, with 28 air changes/hour and 12/12-h light/dark cycle. At the end of experiments (13-14 months of age), echocardiography was performed, followed by cardiac tissue harvests. All animal experiments were approved by the University of Washington Institutional Animal Care and Use Committee.

Echocardiography

Echocardiography was performed as described (Dai *et al*. 2009) using Siemens Acuson CV-70 equipped with 13MHz probe. Isoflurane 0.5% mixed with O_2 was applied to provide adequate sedation while minimizing cardiac suppression during echocardiography. M-mode, conventional and Tissue Doppler, and functional calculations were performed according to

American Society of Echocardiography guidelines. MPI was calculated as the ratio of the sum of isovolemic contraction and relaxation time to LV ejection time. An increase in MPI is an indication that a greater fraction of systole is spent to cope with the pressure changes during isovolemic phases, which has been shown to be a sign of LV systolic and diastolic dysfunction(Dai *et al*. 2009).

Quantitative Pathology

Quantitative histopathology was performed as previously described (Dai *et al*. 2009). In brief, transverse slices of heart tissue were paraffin-embedded, sectioned, and subjected to Masson Trichrome. The percentage of blue-staining fibrotic tissue was measured relative to the total cross-sectional area of the ventricles. Mean myocardial fiber width was determined using 250-350 longitudinally-oriented cardiomyocytes per sample, as visualized from 4-5 high-power (400X) microscopic images.

Measurement of mitochondrial protein carbonyl groups

Ventricular tissue samples were homogenized on ice in mitochondrial isolation buffer (sucrose 250mM, 1mM EGTA, 10mM HEPES, 10mM Tris-Hcl, pH7.4). The lysates were centrifuged at 800g for 7 minutes at 4°C. The supernatants were subsequently centrifuged at 4000g for 30 min at 4°C. The crude pellets (mitochondria) were re-suspended in small volume of isolation buffer, sonicated on ice to break the membrane, and treated with 1% streptomycin sulfate to precipitate mitochondrial nucleic acids. An OxiSelect™ Protein Carbonyl ELISA Kit (Cell Biolabs) was used to analyze 1μg of protein sample per assay. The ELISA was performed as described in the kit manual. In short, protein samples were reacted with dinitrophenylhydrazine (DNPH) and probed with anti-DNPH antibody, followed by HRP conjugated secondary antibody. With the exception of diluting the anti-DNPH antibody and the secondary antibody to 1:2500 and 1:4000, respectively, the procedure was followed closely in accordance to the manufacturer's protocol.

The random mutation capture assay of mtDNA deletions was performed as described (Vermulst *et al*. 2008). In short, mitochondria were isolated from ventricular tissues, followed by extraction and purification of mtDNA. TaqI endonuclease was used to digest the mtDNA. Two primer sets were used in real-time PCR. The first set (deletion primers) flanks multiple TaqI restriction sites and is amplified when there is a segmental deletion of all TaqI restriction sites. The second set (controls) amplifies an adjacent region not containing a TaqI restriction site, which quantities the total amount of mtDNA template in the sample. Both WT and mutant molecules are quantified. Deletion frequency is calculated by the amount of mutant molecules normalized to the amount of WT molecules. The primers for deletion assay are AGGCCACCACACTCCTATTG and AATGCTAGGCGTTTGATTGG, and the control forward and reverse primers are TCGGCGTAAAACGTGTCAACT & CCGCCAA GTCCTTTGAGTTT, respectively.

Quantitative PCR

Taqman Gene Expression Assays and Applied Biosystems 7900 thermocycler were used to quantitate the relative gene expressions. The genes include: PGC1-α (Mm00731216), TFAM (Mm00447485), NRF-1 (Mm00447996), NRF-2 (Mm00487471), collagen 1a2 (Mm 00483937), p16 (forward primer CCCAACGCCCCGAACT, reverse primer AACGTTGCCCATCATCATCA, probe 6FAM TTTCGGTCGTACCCCGATMGBNFQ). All expression assays were normalized to 18S RNA.

Western Blot

Ventricular tissue samples were homogenized on cold lysis buffer (1.5mM KCl, 50mM Tris HCl, 0.125% Sodium deoxycholate, 0.375% Triton × 100, 0.15% NP40, 3mM EDTA) containing protease and phosphatase inhibitors on ice. The samples were sonicated and centrifuged at 10,000g for 15 minutes at 4°C. The supernatant was subsequently collected and the concentration was determined using a BCA assay (Pierce BCA Protein Assay Kit, Thermo Scientific, Rockford,IL). Total protein (10μg) was separated on NuPAGE 4-12% Bis-Tris gel (Invitrogen) and transferred to PVDF 0.45μm membrane (Millipore), then blocked with 5% non-fat dry milk in Tris-buffer solution containing 0.1% Tween-20 for 1 hour. Membranes were incubated with primary antibodies overnight at 4°C. The primary antibodies include: rabbit monoclonal anti-cleaved caspase-3 (Cell Signaling) and mouse monoclonal anti-GAPDH (Millipore). After thorough washes with tris-buffer containing 0.1%Tween-20, membranes were incubated with their corresponding secondary antibodies for 1 hour. Detection was achieved using the enhanced chemiluminescence method (Thermo Scientific). Image Quant ver.2.0 was used to quantified the relative band density as a ratio to GAPDH (internal control). All samples were normalized to the same cardiac protein sample.

Statistical Analysis

All data with normal distribution were presented as means±SEM. Skewed data were presented as boxplot (25%, median and 75% for the box). ANOVA was used to compare differences among multiple groups, followed by Tukey post-hoc analysis to specifically test the significance between WT vs. $Polg^{m/m}$ and $Polg^{m/m}$ vs. $Polg^{m/m}$/mCAT. For skewed data, logarithmic transformation was done followed by two-sample Student *t*-tests to compare between two groups. Stata IC version 10 was used for statistical analysis. $P<0.05$ was considered significant.

Acknowledgments

This work was supported by National Institute of Health Grants P30 AG013280, P01 AG001751 and R01 AG028455

References

Arany Z, He H, Lin J, Hoyer K, Handschin C, Toka O, Ahmad F, Matsui T, Chin S, Wu PH, Rybkin II, Shelton JM, Manieri M, Cinti S, Schoen FJ, Bassel-Duby R, Rosenzweig A, Ingwall JS, Spiegelman BM. Transcriptional coactivator PGC-1 alpha controls the energy state and contractile function of cardiac muscle. Cell Metab. 2005; 1:259–271. [PubMed: 16054070]

Balaban RS, Nemoto S, Finkel T. Mitochondria, oxidants, and aging. Cell. 2005; 120:483–495. [PubMed: 15734681]

Collado M, Blasco MA, Serrano M. Cellular senescence in cancer and aging. Cell. 2007; 130:223–233. [PubMed: 17662938]

Corral-Debrinski M, Horton T, Lott MT, Shoffner JM, Beal MF, Wallace DC. Mitochondrial DNA deletions in human brain: regional variability and increase with advanced age. Nat Genet. 1992; 2:324–329. [PubMed: 1303288]

Dai DF, Santana LF, Vermulst M, Tomazela DM, Emond MJ, MacCoss MJ, Gollahon K, Martin GM, Loeb LA, Ladiges WC, Rabinovitch PS. Overexpression of catalase targeted to mitochondria attenuates murine cardiac aging. Circulation. 2009; 119:2789–2797. [PubMed: 19451351]

DiMauro S, Schon EA. Mitochondrial respiratory-chain diseases. N Engl J Med. 2003; 348:2656–2668. [PubMed: 12826641]

Goffart S, von Kleist-Retzow J-C, Wiesner RJ. Regulation of mitochondrial proliferation in the heart: power-plant failure contributes to cardiac failure in hypertrophy. Cardiovascular Research. 2004; 64:198–207. [PubMed: 15485678]

Hansen AB, Griner NB, Anderson JP, Kujoth GC, Prolla TA, Loeb LA, Glick E. Mitochondrial DNA integrity is not dependent on DNA polymerase-beta activity. DNA Repair (Amst). 2006; 5:71–79. [PubMed: 16165404]

Herbst A, Pak JW, McKenzie D, Bua E, Bassiouni M, Aiken JM. Accumulation of mitochondrial DNA deletion mutations in aged muscle fibers: evidence for a causal role in muscle fiber loss. J Gerontol A Biol Sci Med Sci. 2007; 62:235–245. [PubMed: 17389720]

Hockenbery DM, Oltvai ZN, Yin XM, Milliman CL, Korsmeyer SJ. Bcl-2 functions in an antioxidant pathway to prevent apoptosis. Cell. 1993; 75:241–251. [PubMed: 7503812]

Ito K, Hirao A, Arai F, Takubo K, Matsuoka S, Miyamoto K, Ohmura M, Naka K, Hosokawa K, Ikeda Y, Suda T. Reactive oxygen species act through p38 MAPK to limit the lifespan of hematopoietic stem cells. Nat Med. 2006; 12:446–451. [PubMed: 16565722]

Khaidakov M, Heflich RH, Manjanatha MG, Myers MB, Aidoo A. Accumulation of point mutations in mitochondrial DNA of aging mice. Mutat Res. 2003; 526:1–7. [PubMed: 12714177]

Kraytsberg Y, Simon DK, Turnbull DM, Khrapko K. Do mtDNA deletions drive premature aging in mtDNA mutator mice? Aging Cell. 2009; 8:502–506. [PubMed: 19416127]

Krishnamurthy J, Torrice C, Ramsey MR, Kovalev GI, Al-Regaiey K, Su L, Sharpless NE. Ink4a/Arf expression is a biomarker of aging. J Clin Invest. 2004; 114:1299–1307. [PubMed: 15520862]

Kujoth GC, Hiona A, Pugh TD, Someya S, Panzer K, Wohlgemuth SE, Hofer T, Seo AY, Sullivan R, Jobling WA, Morrow JD, Van Remmen H, Sedivy JM, Yamasoba T, Tanokura M, Weindruch R, Leeuwenburgh C, Prolla TA. Mitochondrial DNA mutations, oxidative stress, and apoptosis in mammalian aging. Science. 2005; 309:481–484. [PubMed: 16020738]

Lakatta EG, Levy D. Arterial and cardiac aging: major shareholders in cardiovascular disease enterprises: Part II: the aging heart in health: links to heart disease. Circulation. 2003; 107:346–354. [PubMed: 12538439]

Marin-Garcia J, Goldenthal MJ, Moe GW. Abnormal cardiac and skeletal muscle mitochondrial function in pacing-induced cardiac failure. Cardiovasc Res. 2001; 52:103–110. [PubMed: 11557238]

Metodiev MD, Lesko N, Park CB, Camara Y, Shi Y, Wibom R, Hultenby K, Gustafsson CM, Larsson NG. Methylation of 12S rRNA is necessary for in vivo stability of the small subunit of the mammalian mitochondrial ribosome. Cell Metab. 2009; 9:386–397. [PubMed: 19356719]

Mott JL, Zhang D, Freeman JC, Mikolajczak P, Chang SW, Zassenhaus HP. Cardiac disease due to random mitochondrial DNA mutations is prevented by cyclosporin A. Biochem Biophys Res Commun. 2004; 319:1210–1215. [PubMed: 15194495]

Mott JL, Zhang D, Stevens M, Chang S, Denniger G, Zassenhaus HP. Oxidative stress is not an obligate mediator of disease provoked by mitochondrial DNA mutations. Mutat Res. 2001; 474:35–45. [PubMed: 11239961]

Orrenius S, Gogvadze V, Zhivotovsky B. Mitochondrial oxidative stress: implications for cell death. Annu Rev Pharmacol Toxicol. 2007; 47:143–183. [PubMed: 17029566]

Ramsey MR, Sharpless NE. ROS as a tumour suppressor? Nat Cell Biol. 2006; 8:1213–1215. [PubMed: 17077852]

Ressler S, Bartkova J, Niederegger H, Bartek J, Scharffetter-Kochanek K, Jansen-Durr P, Wlaschek M. p16INK4A is a robust in vivo biomarker of cellular aging in human skin. Aging Cell. 2006; 5:379–389. [PubMed: 16911562]

Saffitz JE. Arrhythmogenic cardiomyopathy and abnormalities of cell-to-cell coupling. Heart Rhythm. 2009; 6:S62–65. [PubMed: 19541548]

Schriner SE, Linford NJ, Martin GM, Treuting P, Ogburn CE, Emond M, Coskun PE, Ladiges W, Wolf N, Van Remmen H, Wallace DC, Rabinovitch PS. Extension of murine life span by overexpression of catalase targeted to mitochondria. Science. 2005; 308:1909–1911. [PubMed: 15879174]

Scorrano L, Oakes SA, Opferman JT, Cheng EH, Sorcinelli MD, Pozzan T, Korsmeyer SJ. BAX and BAK regulation of endoplasmic reticulum Ca2+: a control point for apoptosis. Science. 2003; 300:135–139. [PubMed: 12624178]

Sebastiani M, Giordano C, Nediani C, Travaglini C, Borchi E, Zani M, Feccia M, Mancini M, Petrozza V, Cossarizza A, Gallo P, Taylor RW, d'Amati G. Induction of mitochondrial biogenesis is a

maladaptive mechanism in mitochondrial cardiomyopathies. J Am Coll Cardiol. 2007; 50:1362–1369. [PubMed: 17903636]

St-Pierre J, Drori S, Uldry M, Silvaggi JM, Rhee J, Jager S, Handschin C, Zheng K, Lin J, Yang W, Simon DK, Bachoo R, Spiegelman BM. Suppression of reactive oxygen species and neurodegeneration by the PGC-1 transcriptional coactivators. Cell. 2006; 127:397–408. [PubMed: 17055439]

Stein M, Noorman M, van Veen TA, Herold E, Engelen MA, Boulaksil M, Antoons G, Jansen JA, van Oosterhout MF, Hauer RN, de Bakker JM, van Rijen HV. Dominant arrhythmia vulnerability of the right ventricle in senescent mice. Heart Rhythm. 2008; 5:438–448. [PubMed: 18313604]

Szalai G, Krishnamurthy R, Hajnoczky G. Apoptosis driven by IP(3)-linked mitochondrial calcium signals. Embo J. 1999; 18:6349–6361. [PubMed: 10562547]

Takahashi A, Ohtani N, Yamakoshi K, Iida S, Tahara H, Nakayama K, Nakayama KI, Ide T, Saya H, Hara E. Mitogenic signalling and the p16INK4a-Rb pathway cooperate to enforce irreversible cellular senescence. Nat Cell Biol. 2006; 8:1291–1297. [PubMed: 17028578]

Trifunovic A, Wredenberg A, Falkenberg M, Spelbrink JN, Rovio AT, Bruder CE, Bohlooly YM, Gidlof S, Oldfors A, Wibom R, Tornell J, Jacobs HT, Larsson NG. Premature ageing in mice expressing defective mitochondrial DNA polymerase. Nature. 2004; 429:417–423. [PubMed: 15164064]

Ventura-Clapier R, Garnier A, Veksler V. Transcriptional control of mitochondrial biogenesis: the central role of PGC-1alpha. Cardiovasc Res. 2008; 79:208–217. [PubMed: 18430751]

Vermulst M, Bielas JH, Kujoth GC, Ladiges WC, Rabinovitch PS, Prolla TA, Loeb LA. Mitochondrial point mutations do not limit the natural lifespan of mice. Nat Genet. 2007; 39:540–543. [PubMed: 17334366]

Vermulst M, Wanagat J, Kujoth GC, Bielas JH, Rabinovitch PS, Prolla TA, Loeb LA. DNA deletions and clonal mutations drive premature aging in mitochondrial mutator mice. Nat Genet. 2008; 40:392–394. [PubMed: 18311139]

Wanagat J, Wolff MR, Aiken JM. Age-associated changes in function, structure and mitochondrial genetic and enzymatic abnormalities in the Fischer 344 × Brown Norway F(1) hybrid rat heart. J Mol Cell Cardiol. 2002; 34:17–28. [PubMed: 11812161]

Wang W, Chen JX, Liao R, Deng Q, Zhou JJ, Huang S, Sun P. Sequential activation of the MEK-extracellular signal-regulated kinase and MKK3/6-p38 mitogen-activated protein kinase pathways mediates oncogenic ras-induced premature senescence. Mol Cell Biol. 2002; 22:3389–3403. [PubMed: 11971971]

Wu Z, Puigserver P, Andersson U, Zhang C, Adelmant G, Mootha V, Troy A, Cinti S, Lowell B, Scarpulla RC, Spiegelman BM. Mechanisms controlling mitochondrial biogenesis and respiration through the thermogenic coactivator PGC-1. Cell. 1999; 98:115–124. [PubMed: 10412986]

Zhang D, Mott JL, Farrar P, Ryerse JS, Chang SW, Stevens M, Denniger G, Zassenhaus HP. Mitochondrial DNA mutations activate the mitochondrial apoptotic pathway and cause dilated cardiomyopathy. Cardiovasc Res. 2003; 57:147–157. [PubMed: 12504824]

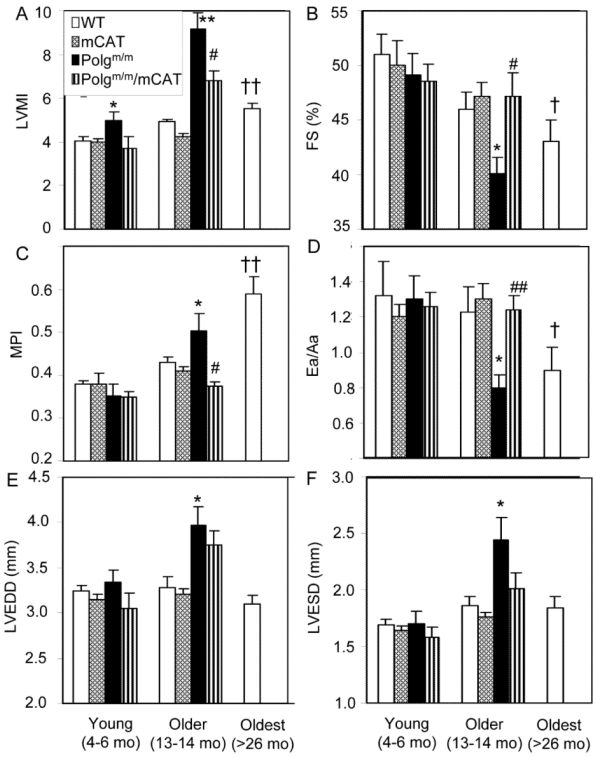

Fig. 1.

Echocardiography of older mice (13-14 months old) showed that Polg$^{m/m}$ mice had increased LV mass, enlarged chamber and depressed contractility, which were attenuated by overexpression of mCAT. Compared with older WT littermates, older Polg$^{m/m}$ mice showed marked increase in LV mass index (A), significant impairment of fractional shortening (B), myocardial performance index (C) and diastolic function shown by Ea/Aa <1 (D), all of which were significantly attenuated in older Polg$^{m/m}$ mice overexpressing mCAT. LV chamber significantly enlarged for both end-diastolic and end-systolic phase (E,F). LVEDD: LV end-diastolic diameter, ESD: end-systolic diameter. *n*=5-8 each group. **P*<0.05, ***P*<0.01 for Polg$^{m/m}$ vs. WT littermates, #*P*<0.05, ##*P*<0.01 for Polg$^{m/m}$ vs. Polg$^{m/m}$/mCAT. †*P*<0.05, ‡ *P*<0.01 for oldest WT vs. young WT.Note: Data from the oldest mice data were obtained by reanalyzing our previous mCAT cohort, n=20 (Dai *et al*. 2009).

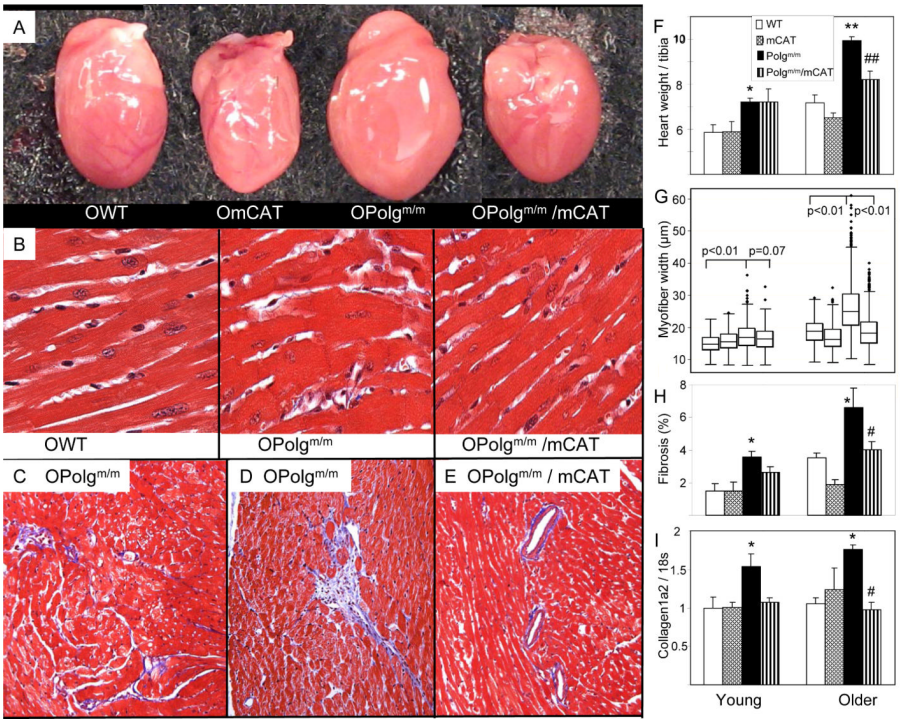

Fig. 2.

Polg$^{m/m}$ induced age-dependent cardiac hypertrophy as seen by increased heart dimension (A), increased heart weight normalized to tibia length (F) and enlarged cardiomyocytes width (B,G), all of which were significantly attenuated by mCAT overexpression. Representative fields stained with Masson's trichrome from older Polg$^{m/m}$ mouse ventricles demonstrated mild interstitial fibrosis (D) and foci of replacement fibrosis (E), while older Polg$^{m/m}$/mCAT littermate mice showed only very minimal perivascular fibrosis (C). (H).Quantitative analysis of the blue-staining fibrotic area on the trichrome-stained sections revealed a significant increase in ventricular fibrosis in the Polg$^{m/m}$ hearts relative to control or mCAT hearts, n=6-8 each group. (I).Quantitative PCR showed significant increase of procollagen type 1α2 expression in Polg$^{m/m}$ mouse ventricles, which is protected in Polg$^{m/m}$/mCAT. *P<0.05, **P<0.01 for Polg$^{m/m}$ vs. WT, #P<0.05, ##P<0.01 for Polg$^{m/m}$ vs. Polg$^{m/m}$/mCAT; n=6-9 each group

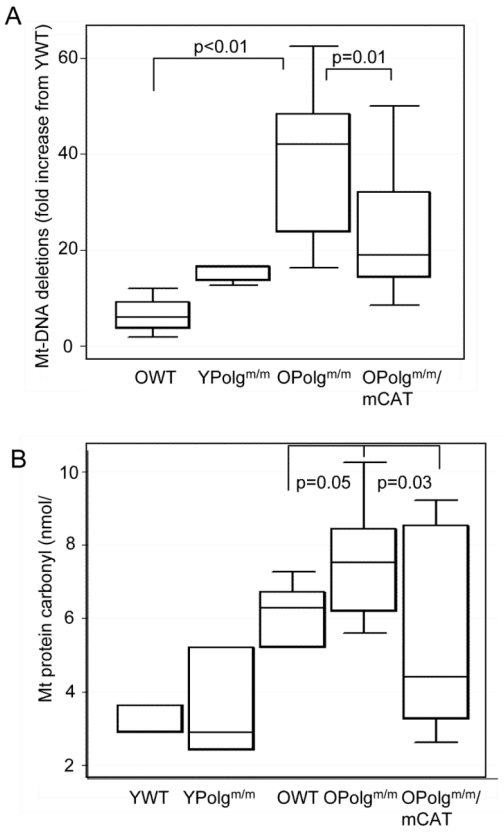

Fig. 3.

Mitochondrial oxidative damage in older Polg$^{m/m}$ was attenuated by mCAT overexpression. (A) Protein carbonyl content was quantified using a DNPH-based enzyme immunoassay of cardiac mitochondrial protein extracts. Older Polg$^{m/m}$ had higher protein carbonylation in cardiac mitochondrial protein extract when compared with WT littermates (P=0.05), and this was partially protected in mCAT mice (P=0.03) (B). Mitochondrial DNA deletion frequencies quantified by random mutation capture assay showed approximately 10-fold increase in Older Polg$^{m/m}$ as compared with WT littermates (P<0.001), and this was substantially attenuated in Polg$^{m/m}$/mCAT mouse hearts (P=0.013). n=4-6 for controls, n= 10-14 for older Polg$^{m/m}$ and Polg$^{m/m}$/mCAT. Note: the bottom, middle and top lines of the box represent the 25th, 50th (median) and 75th percentiles.

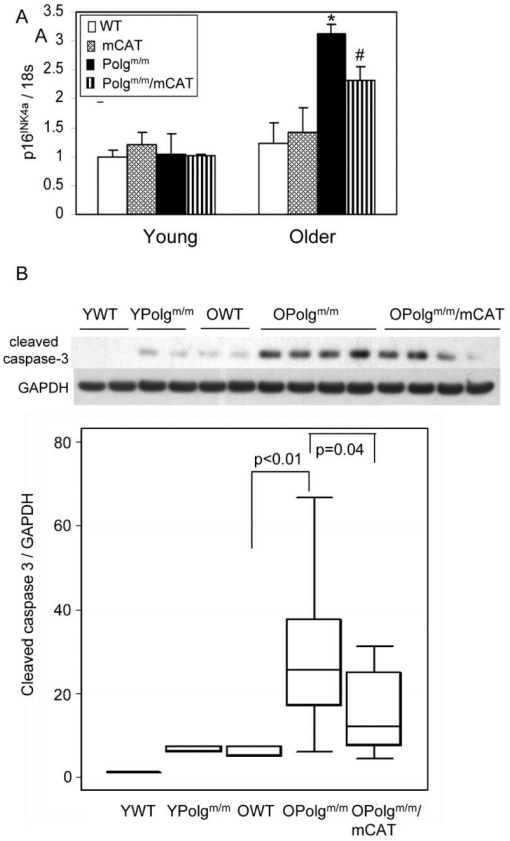

Fig.4.

Senescence and apoptosis markers increased in older Polg$^{m/m}$ mouse hearts. (A). Expression analysis revealed approximately 3-fold increase in p16 expression in older Polg$^{m/m}$ when compared with WT littermates (*P*=0.02), and this is attenuated by mCAT overexpression (*P*=0.03), n=6-9 each group. (B). Activated caspase-3 quantified by Western blot demonstrated a greater than 5-fold increase in older Polg$^{m/m}$ hearts, when compared with WT littermates (*P*<0.001), and this was significantly reduced by 2-fold in Polg$^{m/m}$/mCAT (*P*=0.04). n=3 for controls, n=9-10 for older Polg$^{m/m}$ and Polg$^{m/m}$/mCAT

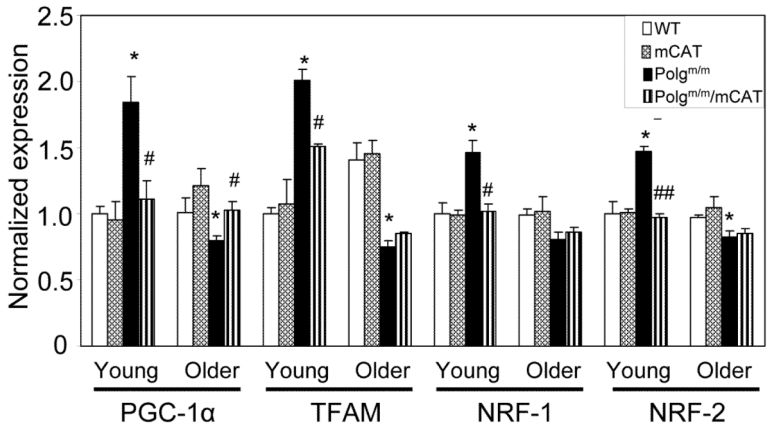

Fig 5.

Expression of genes implicated in mitochondrial biogenesis was significantly increased in young Polg$^{m/m}$ hearts (P<0.05 for all of the above genes when compared with YWT), and was attenuated in young Polg$^{m/m}$/mCAT. In contrast, PGC-1α and TFAM expression decreased significantly in older Polg$^{m/m}$ and this was attenuated in older Polg$^{m/m}$/mCAT (P=0.02 for PGC-1α and P=0.09 for TFAM). *P<0.05 compared with WT; #P<0.05, ## P<0.01 compared with Polg$^{m/m}$, n=6-9 each group.